Percolation and jamming in random sequential adsorption of linear *k*-mers on square lattices with the presence of impurities

J. Stat. Mech. (2015) P10011

(http://iopscience.iop.org/1742-5468/2015/10/P10011)

Journal of Statistical Mechanics: Theory and Experiment
An IOP and SISSA journal

Percolation and jamming in random sequential adsorption of linear *k*-mers on square lattices with the presence of impurities

P M Centres and A J Ramirez-Pastor

Departamento de Física, Instituto de Física Aplicada, Universidad Nacional de San Luis-CONICET, Ejército de Los Andes 950, D5700HHW, San Luis, Argentina
E-mail: antorami@unsl.edu.ar

Received 30 June 2015
Accepted for publication 26 August 2015
Published 9 October 2015

Online at stacks.iop.org/JSTAT/2015/P10011
doi:10.1088/1742-5468/2015/10/P10011

Abstract. Percolation and jamming of linear k-mers (particles occupying k adjacent sites) on two-dimensional square lattices with impurities have been studied by numerical simulations and finite-size scaling analysis. The model offers a simplified representation of the problem of percolation in amorphous solids, where the presence of defects in the system is simulated by introducing a fraction of imperfect bonds ρ, which are considered forbidden for deposition. The dependence of percolation and jamming thresholds on the concentration of defects was investigated for different values of k, ranging from 2 to 64. The results obtained show that: for each fixed value of k, percolation can occur when ρ is smaller than a certain value ρ_k^*; and in the range $0 \leqslant \rho \leqslant \rho_k^*$, the percolation threshold is practically independent of the fraction of defects. The behavior of ρ_k^* as a function of k indicates that the percolation of linear k-mers on square lattices is impossible even for an ideal lattice if $k \gtrapprox 5500$. Critical exponents were also calculated to show that the universality class corresponding to ordinary percolation is preserved.

Keywords: percolation problems, jamming problems, linear k-mers, disordered lattices

1742-5468/15/P10011+19$33.00

Contents

1. Introduction

Percolation is currently a very active field of research in science and technology [1–3]. In physics, percolation theory has been used to study metal–insulator phase transitions, fluid flow in random media, sol–gel transitions and failures in complex networks, just to mention some applications [1–3]. Percolation models have also been used to understand many chemical, biological and social phenomena [2, 4, 5].

In the classical percolation model, a single lattice site (or a bond connecting two sites) is occupied with probability $\theta \in [0, 1]$ or empty (non-occupied) with probability $1 - \theta$. Nearest-neighbor occupied sites (bonds) form structures called clusters. The main idea of percolation theory is based on finding the minimum concentration of elements (sites or bonds) for which a cluster extends from one side to the other of the lattice. This particular value of the concentration rate is named the critical concentration or percolation threshold θ_c, and determines a phase transition in the system. For the precise value of $\theta = \theta_c$, at least one spanning cluster connects the borders of the system [1]. This geometric transition is a second-order phase transition and can be characterized by well-defined critical exponents.

More general percolation problems can be formulated by including the deposition of k-mers (objects occupying more than one site (bond) on the lattice). Computer simulation of this process is usually realized by using the random sequential adsorption (RSA) procedure. The RSA model is well described in the literature and has been investigated extensively in recent decades [6–10]. In this framework, the quantity of interest is the fraction of lattice sites covered at time t by the deposited particles $\theta(t)$. When extended objects are randomly and irreversibly deposited on a lattice, a limiting or jamming

J. Stat. Mech. (2015) P10011

state is generated in which no more objects can be deposited due to the absence of free space of appropriate size and shape, being $\theta(t \to \infty) \equiv \theta_j < 1$. Accordingly, θ ranges from 0 to θ_j for objects occupying more than one site, and the interplay between RSA and percolation must be considered.

Several important contributions regarding percolation and jamming of k-mers have been reported over the last 25 years [11–19].

In [11], linear k-mers with a length in the interval $k = 1$, ..., 20 were randomly and isotropically deposited on a two-dimensional (2D) square lattice. By computer simulations, the authors found that the percolation threshold decreases with increasing chain length k. A similar behavior was observed by Cornette *et al* [12, 13] for sizes k ranging from 1 to 15. In addition, an exhaustive calculation of the critical exponents revealed that the problem belongs to the random percolation universality class regardless of the size of k used in the experiment.

Leroyer and Pommiers [14] extended the study of linear k-mers on square lattices to larger particle sizes (k values up to 40). The authors found that the percolation threshold initially decreases, goes through a minimum around $k = 13$–15, and then increases as the length of the segments increases. Bonnier *et al* [15] also investigated the deposition of linear k-mers (with k between 2 and 512) on a square lattice and found that the jamming concentration monotonically decreases and tends to 0.660(2) as the length of the rods increases.

Vandewalle *et al* studied percolation and jamming phenomena for straight rigid rods of size k on square lattices [16] and found that, for values of k between 2 and 10, the ratio θ_p/θ_j (θ_p being the percolation threshold) remains constant $\theta_p/\theta_j \approx 0.62$, regardless of the length of the particle. Based on this finding, the authors suggested that both critical phenomena (percolation and jamming) are intimately related.

Kondrat and Pekalski [17] extended the study of [16] to larger lattices (lattice size $L = 30$, 100, 300, 1000 and 2500) and longer objects ($1 \leqslant k \leqslant 2000$). The results obtained revealed that: as reported in [15], jamming coverage decreases monotonically approaching the asymptotic value of $\theta_j = 0.66(1)$ for large values of k; the percolation threshold is a nonmonotonic function of the size k—it decreases for small rod sizes, goes through a minimum around $k = 13$ and finally increases for large segments; and the ratio of the two thresholds θ_p/θ_j has a more complex behavior—after initial growth, it stabilizes between $k = 3$ and $k = 7$, and then grows again.

Lebovka *et al* [18] studied anisotropic RSA of straight rigid rods on 2D square lattices. In this model, vertical and horizontal orientations occur with different probabilities, and the degree of anisotropy of the system can be characterized by an order parameter measuring the difference (normalized) between the number of line segments oriented in the vertical direction and the number of line segments oriented in the horizontal direction. The authors investigated the effect of k-mer alignment on jamming properties and found important differences with respect to the isotropic case. In the limit of isotropic systems (order parameter equal to zero), the results obtained by Lebovka *et al* are in excellent agreement with previous simulation data in [17].

Recently, percolation of partially ordered linear k-mers on square lattices has been intensively studied for values of k varying from 1 to 512 and lattice sizes up to $L = 1024$ k [19]. In the case of isotropic systems, Tarasevich *et al* confirmed that the percolation threshold initially decreases, passes through a minimum at $k = 13$ and then increases

with increasing k. In addition, the authors determined that the percolation phase transition only exists for values of k between 1 and approximately 1.2×10^4. For $k > 1.2 \times 10^4$, percolation cannot occur, even at (maximal) jamming concentration.

In the previously discussed works, the surface was considered to be chemically homogeneous and smooth. However, real systems generally present inhomogeneities due to the irregular arrangement of surface and bulk atoms, the presence of various chemical species, etc, which can significantly affect the structure of the substrate. In contrast to the statistics for simple particles, the degeneracy of arrangements of polyatomic species is strongly influenced by the structure of the lattice space. Hence, it is of interest and of value to enquire as to how a heterogeneous lattice structure influences the main percolation properties of k-mers.

From the theoretical point of view, heterogeneous surfaces are generally modeled by lattices with a fraction of defects (or impurities) [20–24]. Two previous articles from our group [22, 23] were devoted to the study of percolation and jamming properties of extended objects deposited on lattices with the presence of impurities. In [22], the problem of linear k-mers of sites (straight rigid particles occupying k consecutive sites) and self-avoiding walk (SAW) k-mers of sites (chains of k adjacent sites generated by a SAW) deposited on a defective square lattice was studied. The defective lattice was built by randomly selecting a fraction of sites which were considered forbidden for deposition. The problem of linear and SAW k-mers of bonds deposited on square lattices with a fraction of defective bonds was investigated in [23].

In both papers [22, 23], simulations were performed for k-mer sizes ranging from 2 to 9. For each value of k, the results showed the existence of a critical fraction of impurities c_c, above which percolation becomes impossible. Each curve of c_c as a function of k allowed a phase diagram to be built separating a percolation from a non-percolation region. Thus, four phase diagrams were obtained corresponding to linear k-mers of sites, SAW k-mers of sites, linear k-mers of bonds and SAW k-mers of bonds. In all cases, theoretical extrapolations of the curves of $c_c(k)$ indicated that the critical concentration of impurities tends to a finite saturation value for large values of k, $c_c(k \to \infty) =$ finite. These findings would suggest that, even for species of large size, the system has a percolation regime for an appropriate value of impurity concentration.

In a recent paper, Tarasevich *et al* [24] extended the study of linear k-mers of sites on square lattices with defective sites to larger particle sizes (k values up to 128). The authors confirmed the results reported by Cornette *et al* [22] for small k-mer sizes and, based on an accurate extrapolation of the results obtained for large k-mers, found that percolation of k-mers is impossible even for an ideal lattice if the length k exceeds a certain critical value.

In [24], a model of linear k-mers with defects (k-mers containing a fraction of non-conducting defects) on an ideal square lattice was also studied. In this case, k-mer sizes ranging from 2 to 256 were considered. For each size k, a critical concentration of defects was found. Above this concentration, percolation is impossible. The behavior of the critical concentration of defects as a function of k revealed that the percolation of very large k-mers ($k \gtrapprox 6 \times 10^3$) on square lattices is impossible even for ideal k-mers.

In the limit of large values of k, the results in [22–24] are consistent with previous work on homogeneous lattices [11–14, 17, 19]. Namely, numerical simulations for small k-mer sizes and corresponding theoretical extrapolations [11–13] predict the existence

of percolation phase transition in the full range of k; in contrast, extrapolations from computer experiments with larger k-mers [14, 17, 19] indicate that percolation is impossible if k exceeds a certain critical value. Direct confirmation of this conjecture requires very time-consuming simulations for very large k-mers and it is still an open problem.

Despite these recent results, the problem of linear k-mers of sites on lattices with a fraction of defective bonds has not been considered up to now. In this case, the defects represent a variable connectivity, as inspired by the problem of percolation on the surface of amorphous solids. Following this line of thought, a simplified statistical model for percolation of k-mers on the surface of amorphous solids is presented in this contribution. Here, the substrate is represented by a 2D square lattice of M sites and $B = 2M$ bonds connecting neighboring sites. Each bond can be either a regular bond or a defective bond. Defective and regular bonds are randomly distributed with concentration ρ and $1 - \rho$, respectively. In this way, the degree of disorder of the surface is tunable by selecting the value of ρ. Linear k-mers are deposited randomly, sequentially and irreversibly on the substrate with the following restriction: the k consecutive empty sites selected for deposition of a k-mer must be connected by $(k - 1)$ regular bonds.

The paper is organized as follows: the model is described in section 2. The kinetics and jamming coverage are studied in section 3. The percolation properties are presented in section 4: simulation scheme, section 4.1; dependence of the percolation threshold on the size k and the lattice disorder degree ρ, section 4.2; and analysis of the critical exponents and universality class, section 4.3. Finally, conclusions are given in section 5.

2. Model

Let us consider the substrate represented by a 2D square lattice of $M = L \times L$ sites (vertices) and $B = 2M$ bonds connecting neighboring sites. Each bond can be either a regular bond or a defective (or imperfect) bond. Defective and regular bonds are randomly distributed with concentration ρ and $1 - \rho$, respectively (see figure 1). In this way, the degree of disorder of the surface is tunable by selecting the value of ρ. The model offers a simplified representation of an amorphous solid, where the presence of defects in the system is simulated by introducing a fraction of imperfect bonds. In the extreme limit where $\rho = 0$, the ideal homogeneous surface is recovered.

In the filling process, linear k-mers (with $k \geqslant 2$) are deposited randomly, sequentially and irreversibly on an initially empty lattice. The deposition procedure is as follows. Given a lattice of linear dimension L and disorder degree ρ ($L - \rho$ –lattice): (i) one of the two (x, y) possible lattice directions and a starting site are randomly chosen; (ii) if, beginning at the chosen site, there are k consecutive empty sites connected by $(k - 1)$ regular bonds along the direction selected in (i), then a k-mer is deposited on those sites. Otherwise, the attempt is rejected. A Monte Carlo step (MCS) is completed after we repeat (i) and (ii) M times. When N rods are deposited, the concentration is $\theta = kN/M$. Figure 1 shows a typical configuration corresponding to 6 mers (solid circles surrounded by ellipses) on a 10×10 square lattice with $\rho \approx 0.15$ and $\theta = 0.54$. Solid lines represent regular bonds (defective bonds are absent) and crosses correspond to empty sites.

J. Stat. Mech. (2015) P10011

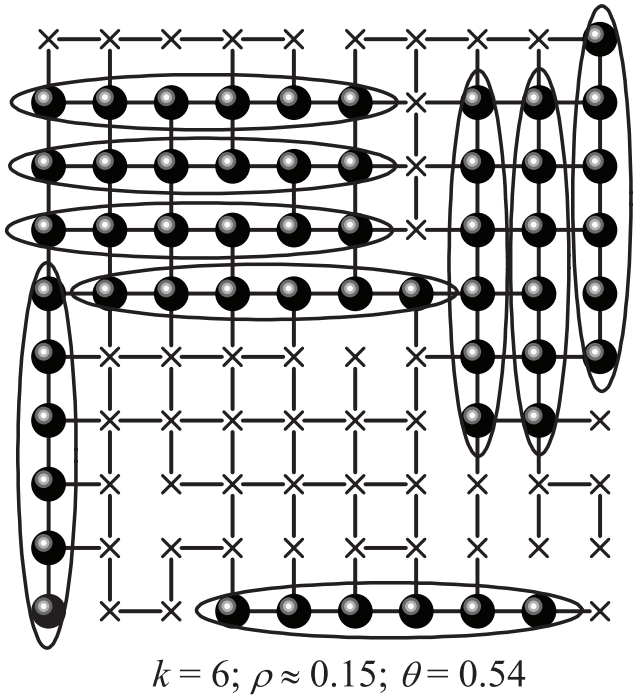

Figure 1. Typical configuration corresponding to 6 mers (solid circles surrounded by ellipses) on a 10×10 square lattice with $\rho \approx 0.15$ and $\theta = 0.54$. Solid lines represent regular bonds (defective bonds are absent) and crosses correspond to empty sites.

3. Kinetics and jamming coverage

Due to blocking of the lattice by the already randomly deposited dimers, the limiting or jamming coverage $\theta_j \equiv \theta(t = \infty)$ is less than that corresponding to the close packing ($\theta_j < 1$). Note that $\theta(t)$ represents the fraction of lattice sites covered at time t by the deposited objects. Consequently, θ ranges from 0 to θ_j for objects occupying more than one site. Jamming coverage depends on the size of the deposited object [10, 15–18, 24] and, in this case, also depends on the degree of disorder of the lattice.

It is well known that it is a quite difficult matter to analytically determine the value of the jamming coverage for a given lattice. For some special types of lattices, geometrical considerations enable their jamming thresholds to be derived exactly [25]. For systems which do not present such a topological advantage, jamming properties have to be estimated numerically by means of computer simulations.

In order to calculate the jamming thresholds, the probability $W_L(\theta)$ that a lattice of linear size L reaches a coverage θ will be used [26]. In the simulations, the procedure to determine $W_L(\theta)$ consists of the following steps: (a) the construction of an $L - \rho$ –lattice (initially empty) and (b) the deposition of particles on the lattice up to the jamming limit θ_j. The jamming limit is reached when it is not possible to adsorb any more k-mers on the surface. In the latter step, the quantity $m_i(\theta)$ is calculated as

$$m_i(\theta) = \begin{cases} 1 & \text{for} \quad \theta \leqslant \theta_j \\ 0 & \text{for} \quad \theta > \theta_j. \end{cases} \tag{1}$$

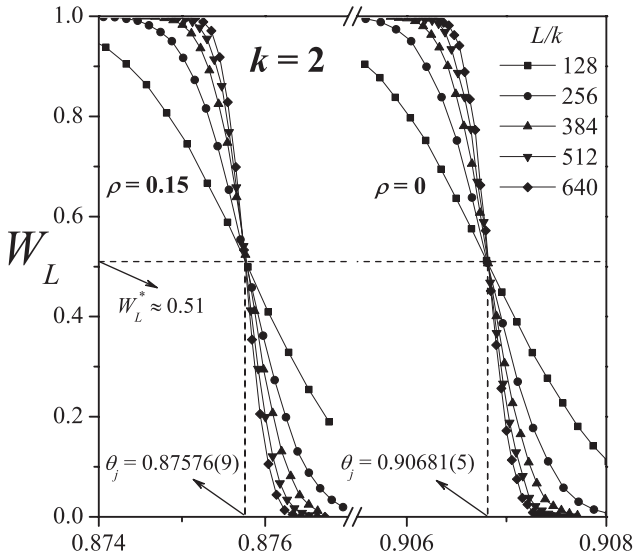

Figure 2. Curves of W_L as a function of the density θ for several values of L/k (as indicated) and two typical cases: $k = 2$ and $\rho = 0$ (right); and $k = 2$ and $\rho = 0.15$ (left). The horizontal dashed line shows the W_L^* point. Vertical dashed lines denote the jamming thresholds in the thermodynamic limit.

n runs of steps (a) and (b) are carried out to obtain the number $m(\theta)$ of them for which a lattice reaches a coverage θ,

$$m(\theta) = \sum_{i=1}^{n} m_i(\theta). \tag{2}$$

Then, $W_L(\theta) = m(\theta)/n$ is defined and the procedure is repeated for different values of L and ρ. A set of $n = 10^5$ independent samples is numerically prepared for several values of the lattice size ($L/k = 128$, 256, 384, 512, 640). The L/k ratio is kept constant to prevent spurious effects due to the k-mer size in comparison with the lattice linear size L. In addition, and given that the system is disordered, all the above calculations are repeated over 100 replicas of the system for each value of ρ, and all quantities are finally averaged over them.

For infinite systems ($L \to \infty$), $W_L(\theta)$ is a step function, being 1 for $\theta \leqslant \theta_j$ and 0 for $\theta > \theta_j$. For finite values of L, $W_L(\theta)$ varies continuously between 1 and 0, with a sharp fall around θ_j. As shown in [26], the jamming coverage can be estimated from the curves of the probabilities W_L plotted versus θ for several lattice sizes. In the vicinity of the limit coverage, the probabilities show a strong dependence on the system size. However, at the jamming point, the probabilities adopt a nontrivial value W_L^*, irrespective of system sizes in the scaling limit. Thus, plotting $W_L(\theta)$ for different linear dimensions L yields an intersection point W_L^*, which gives an accurate estimation of the jamming coverage in the infinite system.

In figure 2, the probabilities $W_L(\theta)$ are shown for different values of L/k (as indicated) and two typical cases: $k = 2$ and $\rho = 0$ (right); and $k = 2$ and $\rho = 0.15$ (left). From inspection of figure 2 (and from data not shown here for the sake of clarity), it can be seen that: for each k and ρ, the curves cross each other at a unique point W_L^*; those points do not modify their numerical value for the different cases studied,

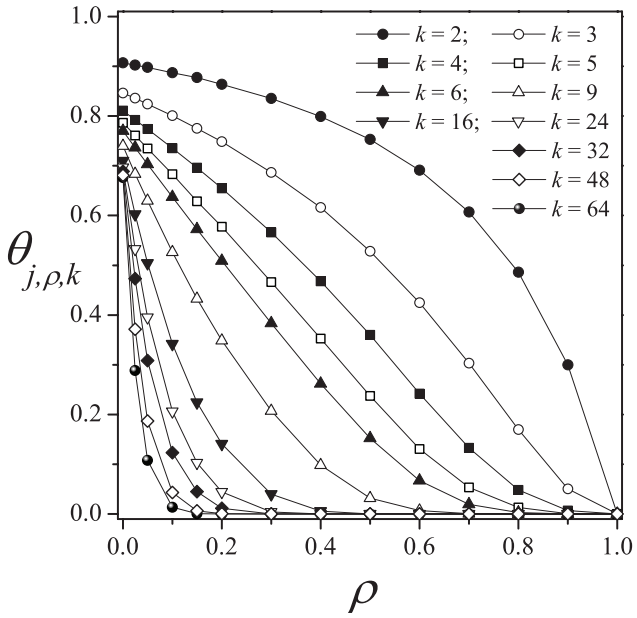

Figure 3. Jamming coverage $\theta_{j,\rho,k}$ as a function of the disorder degree ρ for linear k-mers on square lattices with k between 2 and 64, as indicated. All lines are a guide for the eyes.

being $W_L^* \approx 0.51$; and those points are located at very well defined values in the θ-axes determining the jamming threshold for each k and ρ, $\theta_{j,\rho,k}$. In the case of figure 2, $\theta_{j,\rho=0,k=2} = 0.906\,81(5)$ and $\theta_{j,\rho=0.15,k=2} = 0.875\,76(9)$.

The procedure of figure 2 was repeated for k between 2 and 64, and ρ varying between 0 and 1. The curves corresponding to $k = 24$, $k = 32$, $k = 48$ and $k = 64$ were calculated for $L/k = 128$ and $L/k = 256$, requiring an effort that almost reached the limits of our computational capabilities. The results are shown in figure 3. In the limit of $\rho = 0$, the standard RSA model is recovered and the values obtained of $\theta_{j,\rho,k}$ coincide with those reported in [15–18, 24]. These results validate our program and calculation method.

For each value of k, $\theta_{j,\rho,k}$ decreases as the disorder degree ρ increases. The larger the value of k, the more remarkable the effect is. On the other hand, as k is increased, the values of $\theta_{j,\rho,k}$ decrease over the full range of ρ. This situation can be better visualized in figure 4, where $\theta_{j,\rho,k}$ is plotted as a function of k with ρ as parameter. Extrapolating these values to infinite k-mer size, two well differentiated regimes can be observed. First, for $\rho = 0$, $\theta_{j,\rho=0,k}$ follows the behavior predicted by Bonnier *et al* [15]: $\theta_{j,\rho=0,k} = 0.660 + 1.071/k - 3,47/k^2$ $(k \geqslant 48)$, being $\theta_{j,\rho=0,k=\infty} = 0.660(2)$, the result for the limit coverage of an ideal square lattice by infinitely long k-mers[1]. Second, for $\rho > 0$,

[1] In the case of $\rho = 0$, the values of θ_j obtained in the present paper (k ranging from 2 to 64) improve (one order of magnitude approximately) previous calculations in [15]. With respect to the behavior of the jamming coverage for long k-mers, our results are consistent with the prediction of Bonnier *et al*. [15]. However, more extensive simulations ($k \gg 64$) are required to obtain a more accurate determination of θ_j in the limit of $k \to \infty$. Future work will be conducted in this direction.

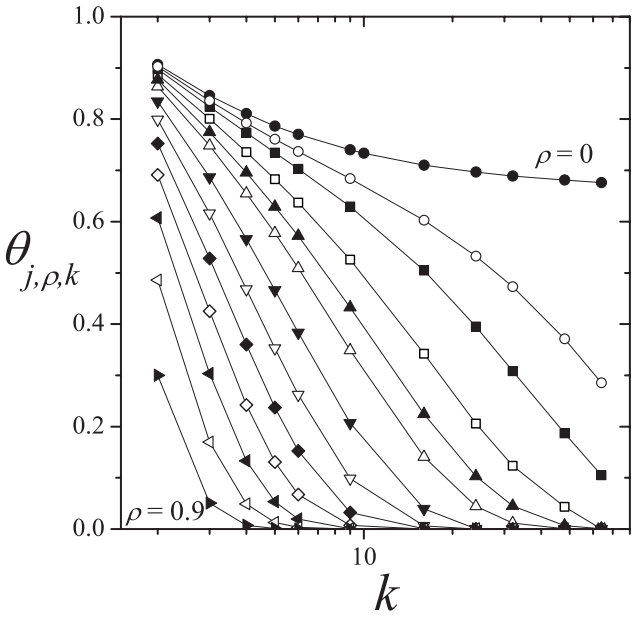

Figure 4. Jamming coverage $\theta_{j,\rho,k}$ as a function of k for different values of the concentration of impurities ρ: $\rho = 0$, solid circles; $\rho = 0.025$, open circles; $\rho = 0.05$, solid squares; $\rho = 0.1$, open squares; $\rho = 0.15$, solid up triangles; $\rho = 0.2$, open up triangles; $\rho = 0.3$, solid down triangles; $\rho = 0.4$, open down triangles; $\rho = 0.5$, solid diamonds; $\rho = 0.6$, open diamonds; $\rho = 0.7$, solid left triangles; $\rho = 0.8$, open left triangles; and $\rho = 0.9$, solid right triangles. All lines are a guide for the eyes.

$\theta_{j,\rho,k}$ tends to 0 as k is increased for all studied values of ρ. In other words, for each value of $\rho > 0$, there exists a finite size $k(\equiv k_0)$ such that $\theta_{j,\rho,k} = 0$ for $k > k_0$.

As explicitly shown in figure 4, $k_0 < 64$ for $0.1 \leqslant \rho \leqslant 1$. In the case of small impurity concentrations, and even though more extensive simulations are required to confirm the existence of the limit value k_0, the curves show a clear change in slope when passing from an ideal system $\rho = 0$ to a disordered system $\rho > 0$ (see the curves corresponding to $\rho = 0.025$ and $\rho = 0.05$). While the saturation value $\theta_{j,\rho=0,k=\infty} = 0.660(2)$ is predicted for $\rho = 0$ and k tending to infinity, a limit value equal to zero is expected for finite k and $\rho > 0$.

4. Percolation

4.1. Simulation scheme

With the space of the parameters θ and ρ determined, the percolation properties of the system will be studied in the following.

As was already mentioned, the central idea of percolation theory is based on finding the minimum concentration θ for which a cluster extends from one side of the system to the other. This particular value of the concentration is called the *critical concentration* or *percolation threshold* and determines a well defined phase transition in the system.

We are interested in determining: the dependence of the percolation threshold on the size k and the lattice disorder degree ρ; and the universality class of the phase transition occurring in the system.

Finite-scaling theory gives us the basis to determine the percolation threshold and the critical exponents of a system with a reasonable accuracy. For this purpose, the probability $R = R^{X}_{L,\rho,k}(\theta)$ that an $L-\rho$ –lattice percolates at a concentration θ of occupied sites by rods of size k can be defined [1, 27, 28]. Here, the following definitions can be given according to the meaning of X:

- $R^{R(D)}_{L,\rho,k}(\theta)$: the probability of finding a rightward (downward) percolating cluster,
- $R^{U}_{L,\rho,k}(\theta)$: the probability of finding either a rightward or a downward percolating cluster,
- $R^{I}_{L,\rho,k}(\theta)$: the probability of finding a cluster that percolates both in a rightward and downward direction, and
- $R^{A}_{L,\rho,k}(\theta) = \frac{1}{2}[R^{U}_{L,\rho,k}(\theta) + R^{I}_{L,\rho,k}(\theta)]$.

Computational simulations were applied to determine each of the previously mentioned quantities. Each simulation run consists of the following steps: the construction of a square lattice of linear size L, disorder degree ρ and coverage θ; and cluster analysis using the Hoshen and Kopelman algorithm [29]. In the latter step, the size of largest cluster S_L is determined, as well as the existence of a percolating island.

A total of $m_{L,\rho}$ independent runs of this two-step procedure were carried out for each lattice size L and disorder degree ρ. From these runs a number $m^{X}_{L,\rho}$ of them present a percolating cluster; this is done for the desired criterion among $X = R, D, I, U, A$. Then, $R^{X}_{L,\rho,k}(\theta) = m^{X}_{L,\rho}/m_{L,\rho}$ is defined and the procedure is repeated for different values of L, θ, ρ and k.

In addition to the different probabilities $R^{X}_{L,\rho,k}(\theta)$, the percolation order parameter P and the corresponding susceptibility χ have been measured [30, 31],

$$P = \langle S_L \rangle / M, \tag{3}$$

and

$$\chi = [\langle S_L^2 \rangle - \langle S_L \rangle^2]/M, \tag{4}$$

where S_L represents the size of the largest cluster and $\langle ... \rangle$ means an average over simulation runs.

In our percolation simulations, we used $m_{L,\rho} = 10^5$ and all the calculations were repeated over 100 replicas of the system. In addition, for each value of θ and ρ, the effect of finite size was investigated by examining square lattices with $L/k = 128$, 256, 384, 512, 640. As can be appreciated, this represents extensive calculations from the computational point of view. From this, finite-scaling theory can be used to determine the percolation threshold and the critical exponents with reasonable accuracy.

J. Stat. Mech. (2015) P10011

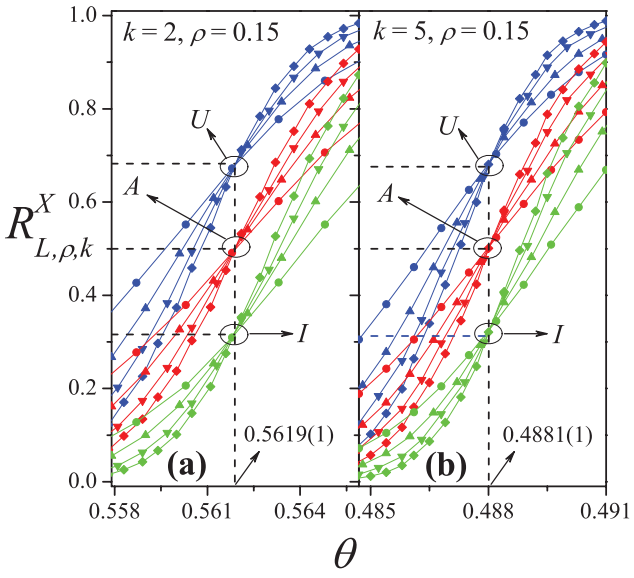

Figure 5. Fraction of percolating lattices $R^X_{L,\rho,k}(\theta)$ ($X = I$, U, A as indicated) as a function of the concentration θ for $k = 2$, $\rho = 0.15$ (a) and $k = 5$, $\rho = 0.15$ (b), and different lattice sizes: $L/k = 256$, circles; $L/k = 384$, up triangles; $L/k = 512$, down triangles; and $L/k = 640$, diamonds. Curves corresponding to $L/k = 128$ are not shown for clarity. The vertical dashed line denotes the percolation threshold $\theta_{c,\rho,k}$ in the thermodynamic limit.

4.2. Percolation threshold

The standard theory of finite-size scaling [1, 27, 28] allows for various efficient routes to estimate the percolation threshold from simulation data. One of these methods, which will be used here, is from the curves of $R^X_{L,\rho,k}(\theta)$.

In figure 5, the probabilities $R^I_{L,\rho,k}(\theta)$, $R^U_{L,\rho,k}(\theta)$ and $R^A_{L,\rho,k}(\theta)$ are presented for two typical cases: (a) $k = 2$ and $\rho = 0.15$ (left); and (b) $k = 5$ and $\rho = 0.15$ (right). In order to express these curves as a function of continuous values of θ, it is convenient to fit $R^X_{L,\rho,k}(\theta)$ with some approximating function through the least-squares method. The fitting curve is the *error function* because $\mathrm{d}R^X_{L,\rho,k}(\theta)/\mathrm{d}\theta$ is expected to behave like the Gaussian distribution [28]

$$\frac{\mathrm{d}R^X_{L,\rho,k}}{\mathrm{d}\theta} = \frac{1}{\sqrt{2\pi}\,\Delta^X_{L,\rho,k}} \exp\left\{-\frac{1}{2}\left[\frac{\theta - \theta^X_{c,\rho,k}(L)}{\Delta^X_{L,\rho,k}}\right]\right\}^2, \tag{5}$$

where $\theta^X_{c,\rho,k}(L)$ is the concentration at which the slope of $R^X_{L,\rho,k}(\theta)$ is the largest and $\Delta^X_{L,\rho,k}$ is the standard deviation from $\theta^X_{c,\rho,k}(L)$.

Once the values of $\theta^X_{c,\rho,k}(L)$ have been obtained for different lattice sizes, a scaling analysis can be conducted [1]. Thus, we have

$$\theta^X_{c,\rho,k}(L) = \theta^X_{c,\rho,k}(\infty) + A^X L^{-1/\nu}, \tag{6}$$

J. Stat. Mech. (2015) P10011

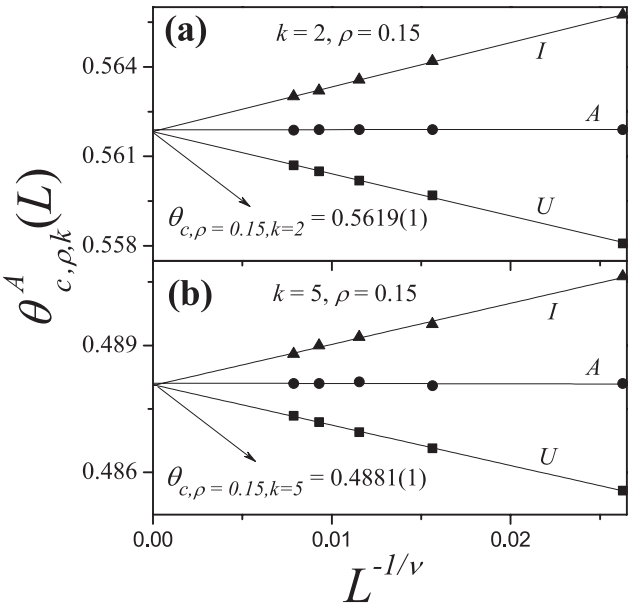

Figure 6. Extrapolation of $\theta^X_{c,\rho,k}(L)$ towards the thermodynamic limit according to the theoretical prediction given by equation (6). Triangles, circles and squares denote the values of $\theta^X_{c,\rho,k}(L)$ obtained by using the criteria I, A and U, respectively. Different values of k and ρ are presented: (a) $k = 2$, $\rho = 0.15$; and (b) $k = 5$, $\rho = 0.15$.

where A^X is a non-universal constant and ν is the critical exponent of the correlation length, which will be taken as 4/3 for the present analysis, since (as will be shown in section 4.3) our model belongs to the same universality class as random percolation [1].

Figure 6 shows plots towards the thermodynamic limit of $\theta^X_{c,\rho,k}(L)$ according to equation (6) for the data in figure 5. From extrapolations it is possible to obtain $\theta^X_{c,\rho,k}(\infty)$ for the criteria I, A and U. Combining the three estimates for each case, the final values of $\theta_{c,\rho,k}(\infty)$ can be obtained. Additionally, the maximum of the differences between $|\theta^U_{c,\rho,k}(\infty) - \theta^A_{c,\rho,k}(\infty)|$ and $|\theta^I_{c,\rho,k}(\infty) - \theta^A_{c,\rho,k}(\infty)|$ gives the error bar for each determination of $\theta_{c,\rho,k}(\infty)$. In this case, the values obtained were: $\theta_{c,\rho=0.15,k=2}(\infty) = 0.5619(1)$ and $\theta_{c,=0.15,k=5}(\infty) = 0.4881(1)$. For the rest of the paper, we will denote the percolation threshold for each size k and each disorder degree ρ by $\theta_{c,\rho,k}$ (for simplicity we will drop the '(∞)').

The procedure of figure 6 was repeated for $k = 2$ and a wide range of values of ρ. The results, which are collected in figure 7, represent the $\theta - \rho$ –phase diagram corresponding to a system of dimers on a square lattice with defective bonds. The curve of $\theta_{c,\rho,k}$ (open circles) extends from the point $[\rho = 0, \theta_{c,\rho=0,k=2} = 0.562(1)]$ on the left to the intersection point between the curves of percolation and jamming thresholds $[\rho^*_{k=2} \approx 0.7355, \theta^*_{k=2} \approx 0.5619]$ (solid star) on the right, where $\theta_{c,\rho=0,k=2} = 0.562(1)$ represents the percolation threshold for dimers on a ideal square lattice, and ρ^*_k corresponds to the critical concentration of defects at which percolation is possible only at jamming coverage.

As reported in [24] for a model of linear k-mers of sites on square lattices with defective sites, the curve of $\theta_{c,\rho,k}$ is almost insensitive to the fraction of impurities ρ. This line

J. Stat. Mech. (2015) P10011

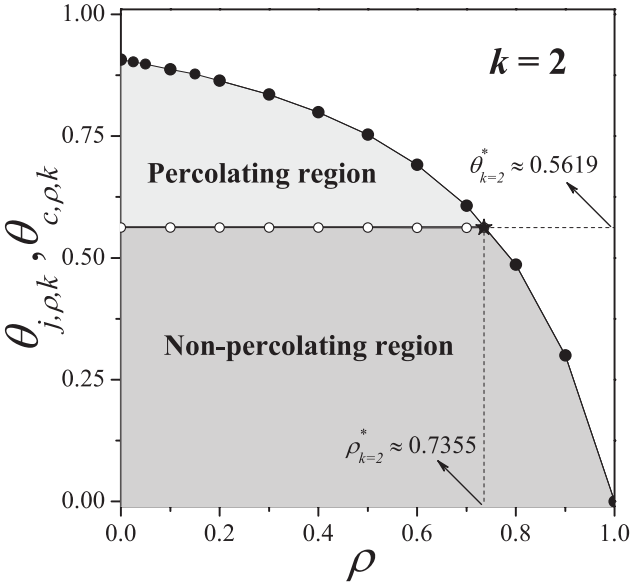

Figure 7. $\theta - \rho$ –phase diagram corresponding to a system of dimers on a square lattice with defective bonds. The curve of $\theta_{c,\rho,k}$ (open circles) divides the space of allowed values of θ in a non-percolating region ($0 < \theta < \theta_{c,\rho,k}$) and a percolating region ($\theta_{c,\rho,k} < \theta < \theta_{j,\rho,k}$). The region above the curve of $\theta_{j,\rho,k}$ (solid circles) corresponds to a forbidden region of the θ-space. The intersection point between the curves of $\theta_{c,\rho,k}$ and $\theta_{j,\rho,k}$ (solid star) corresponds to the critical concentration of defects ρ^*_k at which percolation is possible only at jamming coverage.

divides the space of allowed values of θ in a non-percolating region ($0 < \theta < \theta_{c,\rho,k}$) and a percolating region ($\theta_{c,\rho,k} < \theta < \theta_{j,\rho,k}$). The region above the curve of $\theta_{j,\rho,k}$ (solid circles) corresponds to a forbidden region of the θ-space.

The line separating percolating and non-percolating regions was calculated for k ranging from 2 to 64, and different values of ρ between 0 and ρ^*_k. As mentioned in section 3, the curves corresponding to $k = 24$, $k = 32$, $k = 48$ and $k = 64$ were calculated for $L/k = 128$ and $L/k = 256$. The results are shown in figure 8. The dashed line joins the limit points $[\rho^*_k, \theta^*_k]$. Percolation occurs when ρ is smaller than ρ^*_k, and θ varies between $\theta_{c,\rho,k}$ and $\theta_{j,\rho,k}$.

For a better visualization of the data, the results corresponding to k-mer sizes between 2 and 9 are shown in figure 8(b), and the results corresponding to values of k between 16 and 64 are shown in figure 8(a). The complete curve $\rho^*_k(\theta^*_k)$ is presented in the inset of figure 8(a). As in figure 7, the percolation thresholds are practically independent of the fraction of defects for all values of k. Accordingly, the minimum observed in $\rho^*_k(\theta^*_k)$ reproduces the minimum reported in [19] for the percolation threshold of linear k-mers on homogeneous square lattices.

As k is increased, the length of the interval $[0, \rho^*_k]$ decreases and, consequently, the percolation phase transition tends to disappear. This behavior can be observed more clearly in figure 9, where the dependence of ρ^*_k as a function of k is reported. The results obtained in the present work (blue solid stars) are compared with those reported by Cornette *et al* [22] (red open stars) and Tarasevich *et al* [24] (black solid circles) for

J. Stat. Mech. (2015) P10011

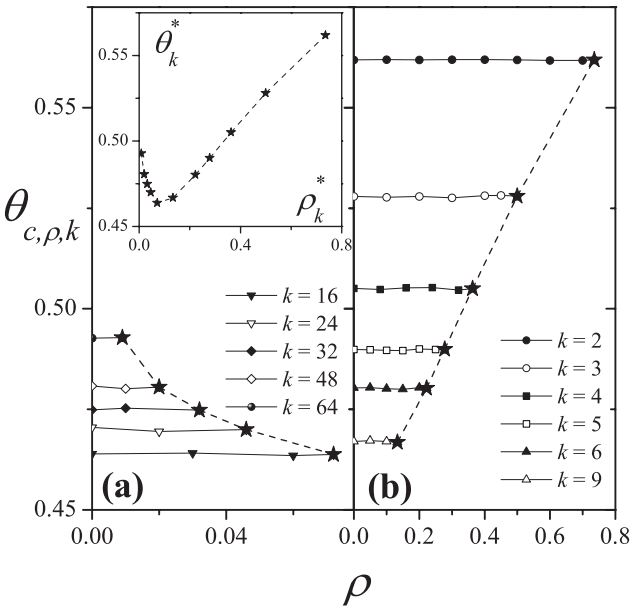

Figure 8. $\theta_{c,\rho,k}$ as a function of ρ for k ranging from 2 to 64, and different values of ρ between 0 and ρ_k^*. The curves corresponding to $k = 16$, $k = 24$, $k = 32$, $k = 48$ and $k = 64$ are shown in part (a) and those corresponding to $k = 2$, $k = 3$, $k = 4$, $k = 5$, $k = 6$ and $k = 9$ are shown in part (b). As discussed in the text, the dashed line joins the limit points $[\rho_k^*, \theta_k^*]$ (stars).

a model of linear k-mers of sites on square lattices with defective sites. As in [24], our simulation data ($2 \leqslant k \leqslant 64$) were fitted by the function

$$\rho_k^* = a\frac{k_m^\alpha - k^\alpha}{b + k^\alpha}, \tag{7}$$

with $a = 0.000\,03 \pm 0.000\,01$, $\alpha = 1.31 \pm 0.04$, $b = 1.04 \pm 0.25$ and $k_m = 5518 \pm 500$. These parameters strongly depend on the smallest value of k used in the fitting (in this case, $k = 2$). In order to analyze the behavior of ρ_k^* for long k-mers, it is more convenient to plot ρ_k^* versus $k^{-\alpha}$ for $k \to k_m$. This is shown in the inset of figure 9, where the solid line corresponds to the linear fit of the simulation data (stars). The value of the critical length estimated from the point at which the solid line cuts the abscissa axis is consistent with that obtained from equation (7).

From an analysis of figure 9, the following conclusions can be drawn. First, for each size k, the corresponding value of ρ_k^* is lower in the case of lattices with defective sites as compared with the case of lattices with defective bonds. This finding indicates that the percolation transition for linear k-mers of sites is more sensitive to the presence of defective lattice sites than defective lattice bonds. Second, the value of k_m obtained in the present work coincides, within numerical error, with the value reported in [24], $k_m = 5900 \pm 500$. Our result reinforces the conjecture that percolation of linear k-mers on square lattices is impossible even for a lattice without any defects if $k \gtrapprox 6 \times 10^3$ [24].

J. Stat. Mech. (2015) P10011

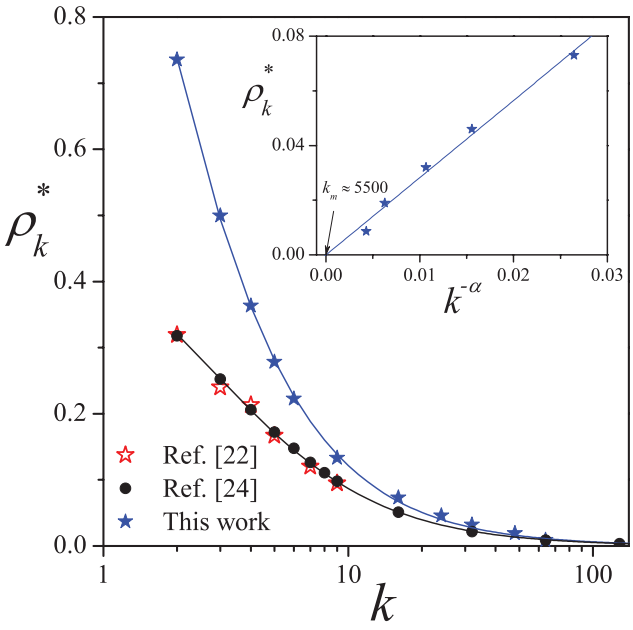

Figure 9. ρ_k^* as a function of k. Comparison of the results obtained in the present work (blue solid stars) and those reported by Cornette *et al* [22] (red open stars) and Tarasevich *et al* [24] (black solid circles) for a model of linear k-mers of sites on square lattices with defective sites. The solid line fitting the simulation data (blue solid stars) corresponds to the function in equation (7). Inset: ρ_k^* versus $k^{-\alpha}$ for $k \to k_m$. The blue solid line corresponds to the linear fit of the simulation data (blue solid stars).

4.3. Critical exponents and universality class

In this section, the critical exponents ν, β and γ will be calculated. Critical exponents are of importance because they describe the universality class of a system and allow related phenomena to be understood.

The standard theory of finite-size scaling allows various methods to be used to estimate ν from numerical data. One of these methods is from the maximum of the function in equation (5) [1],

$$\left(\frac{\mathrm{d}R^X_{L,\rho,k}}{\mathrm{d}\theta}\right)_{\max} \propto L^{1/\nu}. \tag{8}$$

In figure 10(a), $\ln\left[\left(\mathrm{d}R^A_{L,\rho,k}/\mathrm{d}\theta\right)_{\max}\right]$ has been plotted as a function of $\ln[L]$ (note the log–log functional dependence) for the two cases studied in previous figures. According to equation (8) the slope of each line corresponds to $1/\nu$. It can be observed that the slopes of the curves remain constant (and close to 3/4) for all studied cases. Thus, $\nu = 1.36(3)$ for $k = 2$ and $\rho = 0.15$; and $\nu = 1.34(2)$ for $k = 5$ and $\rho = 0.15$. These results coincide, within numerical errors, with the exact value of the critical exponent of ordinary percolation $\nu = 4/3$.

Once we know ν, the exponent γ can be determined by scaling the maximum value of the susceptibility equation (4). According to finite-size scaling theory [1], the behavior

J. Stat. Mech. (2015) P10011

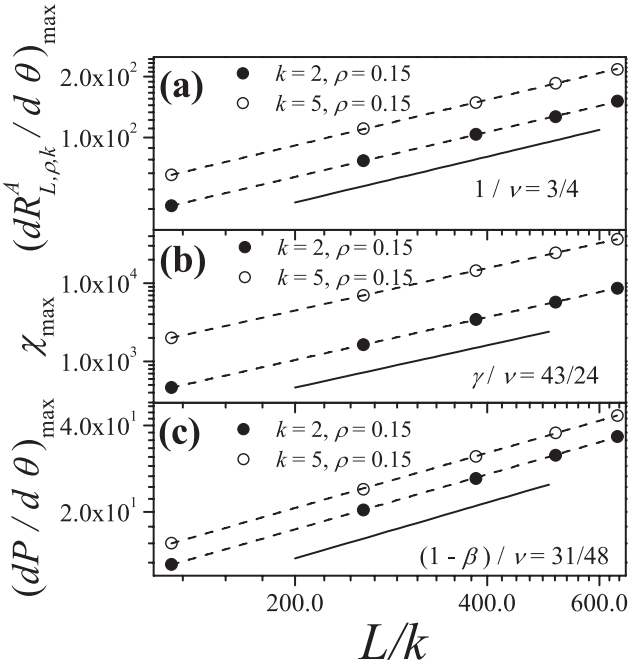

Figure 10. (a) Log–log plot of $(\mathrm{d}R^{A}_{L,\rho,k}/\mathrm{d}\theta)_{\max}$ as a function of L/k for $k=2$, $\rho=0.15$ (solid circles) and $k=5$, $\rho=0.15$ (open circles). According to equation (8) the slope of each line corresponds to $1/\nu=3/4$. (b) Log–log plot of $\chi_{\max}$ as a function of L/k for $k=2$, $\rho=0.15$ (solid circles) and $k=5$, $\rho=0.15$ (open circles). The slope of each line corresponds to $\gamma/\nu=43/24$. (c) Log–log plot of $(\mathrm{d}P/\mathrm{d}\theta)_{\max}$ as a function of L/k for $k=2$, $\rho=0.15$ (solid circles) and $k=5$, $\rho=0.15$ (open circles). According to equation (10), the slope of each curve corresponds to $(1-\beta)/\nu=31/48$.

of χ at criticality is $\chi = L^{\gamma/\nu}\overline{\chi}(u)$, where $u=(\theta-\theta_{c,\rho,k})L^{1/\nu}$ and $\overline{\chi}$ is the corresponding scaling function. At the point where χ is maximal, $u=$ constant and $\chi_{\max}\propto L^{\gamma/\nu}$. Our data for $\chi_{\max}$ are shown in figure 10(b). The values obtained are $\gamma=2.42(4)$ for $k=2$ and $\rho=0.15$; and $\gamma=2.40(3)$ for $k=5$ and $\rho=0.15$. Simulation data are consistent with the exact value of the critical exponent of ordinary percolation, $\gamma=43/18$.

Further to this, the standard way to extract the exponent ratio β is to study the scaling behavior of P at criticality [1],

$$P = L^{-\beta/\nu}\overline{P}(u'), \tag{9}$$

where $u'=|\theta-\theta_{c,\rho,k}|L^{1/\nu}$ and $\overline{P}$ is the scaling function. At the point where $\mathrm{d}P/\mathrm{d}\theta$ is maximal, $u=$ constant and

$$\left(\frac{\mathrm{d}P}{\mathrm{d}\theta}\right)_{\max} = L^{(-\beta/\nu+1/\nu)}\overline{P}(u')\propto L^{(1-\beta)/\nu}. \tag{10}$$

The scaling of $(\mathrm{d}P/\mathrm{d}\theta)_{\max}$ is shown in figure 10(c). From the slopes of the curves, the following values of β were obtained: $\beta=0.15(2)$ for $k=2$ and $\rho=0.15$; and $\beta=0.15(2)$ for $k=5$ and $\rho=0.15$. These results agree very well with the exact value of β for ordinary percolation, $\beta=5/36$.

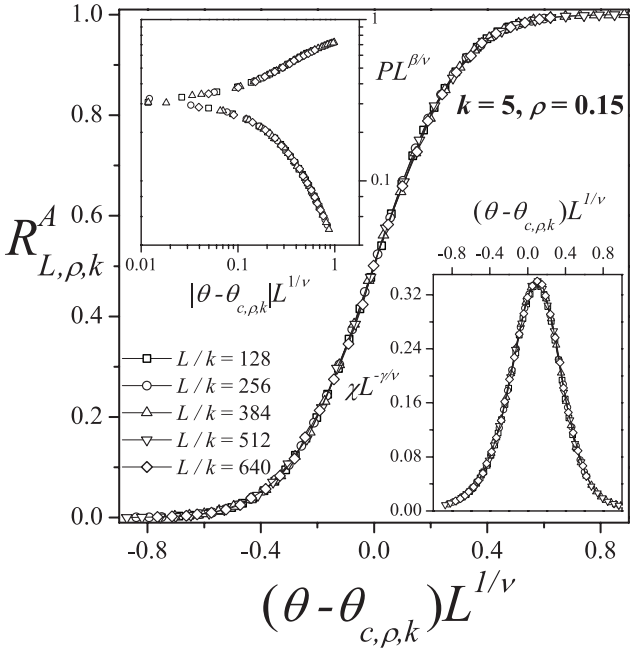

Figure 11. Data collapsing of the percolation probability, $R^A_{L,\rho,k}(\theta)$ versus $(\theta-\theta_{c,\rho,k})L^{1/\nu}$, for $k=5$ and $\rho=0.15$. Upper left inset: data collapsing of the percolation order parameter, $PL^{\beta/\nu}$ versus $|\theta-\theta_{c,\rho,k}|L^{1/\nu}$, for $k=5$ and $\rho=0.15$. Bottom right inset: data collapsing of the susceptibility, $\chi L^{-\gamma/\nu}$ versus $(\theta-\theta_{c,\rho,k})L^{1/\nu}$, for $k=5$ and $\rho=0.15$. The plots were made using $\theta_{c,\rho=0.15,k=5}=0.4881$ and the exact percolation exponents $\nu=4/3$, $\beta=5/36$ and $\gamma=43/18$.

The protocol described in figure 10 was repeated for k between 2 and 64, and ρ varying between 0 and ρ_k^* (these data are not shown here for brevity). In all cases, the values obtained for ν, γ and β clearly indicate that, independently of the size k and the disorder degree ρ, this problem belongs to the same universality class as random percolation.

Scaling behavior can be further tested by plotting $R^X_{L,\rho,k}(\theta)$ versus $(\theta-\theta_{c,\rho,k})L^{1/\nu}$, $PL^{\beta/\nu}$ versus $|\theta-\theta_{c,\rho,k}|L^{1/\nu}$ and $\chi L^{-\gamma/\nu}$ versus $(\theta-\theta_{c,\rho,k})L^{1/\nu}$ and looking for data collapsing [1]. Figure 11 shows the excellent collapse of curves of $R^A_{L,\rho,k}$, P (upper left inset) and χ (bottom right inset) for a typical case ($k=5$ and $\rho=0.15$) and different lattice sizes, as indicated. The plots were made using the value $\theta_{c,\rho=0.15,k=5}=0.4881(1)$ calculated above and the exact values of the critical exponents of ordinary percolation $\nu=4/3$, $\beta=5/36$ and $\gamma=43/18$. This leads to independent controls and consistency checks of the values of all the critical exponents.

5. Conclusions

Percolation and jamming properties in RSA of linear k-mers on square lattices with the presence of impurities have been studied by numerical simulations and finite-size

scaling analysis. The contaminated lattice was built by randomly selecting a fraction of bonds (ρ) of the lattice that were considered forbidden for deposition. The model offers a simplified representation of the problem of percolation in amorphous solids, where the presence of defects in the system is simulated by introducing a fraction of defective bonds.

The dependence of jamming coverage $\theta_{j,\rho,k}$ on disorder degree ρ was studied for k ranging from 2 to 64. $\theta_{j,\rho,k}$ decreases as the fraction of impurities increases for a fixed value of k; and $\theta_{j,\rho,k}$ is a monotonic decreasing function of k for a fixed value of ρ. In the latter case, two well differentiated regimes were observed: for $\rho = 0$, $\theta_{j,\rho=0,k}$ follows the behavior reported by Bonnier *et al* [15], with a finite value of saturation in the limit of infinitely long k-mers, $\theta_{j,\rho=0,k=\infty} = 0.660(2)$; and for $\rho > 0$, $\theta_{j,\rho,k}$ tends to 0 as k is increased and there exists a finite size $k(\equiv k_0)$ such that $\theta_{j,\rho,k} = 0$ for $k > k_0$.

Once the space of the parameters θ and ρ had been determined, complete percolation phase diagrams were obtained for values of k between 2 and 64. The main characteristics of the phase diagrams are the following. The jamming coverage plays an important role in the system considered here. In fact, the curve of $\theta_{c,\rho,k}$ as a function of ρ, which divides the space of allowed values of θ in a non-percolating region and a percolating region, is limited only by the envelope function $\theta_{j,\rho,k}$, being almost insensitive to the concentration of defects. Thus, percolation can occur when ρ is smaller than a certain value ρ_k^*, where ρ_k^* is the fraction of impurities at which the curves of $\theta_{c,\rho,k}$ and $\theta_{j,\rho,k}$ intersect.

Analysis of the dependence of ρ_k^* as a function of k revealed that there exists a finite value $k_m = 5518 \pm 500$ such that $\rho_{k_m}^* = 0$. The value of k_m obtained in the present work coincides, within numerical error, with the value reported in [24] for a system of linear k-mers deposited on a square lattice with defective sites. Our result reinforces the conjecture that percolation of linear k-mers on square lattices is impossible even for a lattice without any defects if $k \gtrapprox 6 \times 10^3$ [24]. However, more simulations are necessary in order to obtain direct confirmation of this conjecture.

Finally, accurate determination of the critical exponents revealed that the problem belongs to the same universality class as random percolation regardless of the values of ρ and k considered.

Acknowledgments

This work was supported in part by CONICET (Argentina) under project number PIP 112-201101-00615; Universidad Nacional de San Luis (Argentina) under project 322000; and the National Agency of Scientific and Technological Promotion (Argentina) under project PICT-2013-1678. The numerical work was conducted using the BACO parallel cluster (composed of 70 PCs each with an Intel i7-3370 / 2600 processor) located at the Instituto de Física Aplicada, Universidad Nacional de San Luis—CONICET, San Luis, Argentina.

References

[1] Stauffer D and Aharony A 1994 *Introduction to Percolation Theory* (London: Taylor and Francis)
[2] Sahimi M 1994 *Applications of Percolation* (London: Taylor and Francis)

J. Stat. Mech. (2015) P10011

[3] Bollobás B and Riordan O 2006 *Percolation* (New York: Cambridge University Press)
[4] Shao J, Havlin S and Stanley H E 2009 *Phys. Rev. Lett.* **103** 018701
[5] Goldenberg J, Libai B, Solomon S, Jan N and Stauffer D 2000 *Physica* A **284** 335
[6] Feder J 1980 *J. Theor. Biol.* **87** 237
[7] Barlelt M C and Privman V 1990 *J. Chem. Phys.* **93** 6820
[8] Manna S and Svarakic N M 1991 *J. Phys.* A **24** L671
[9] Privman V, Wang J-S and Nielaba P 1991 *Phys. Rev.* B **43** 3366
[10] Evans J W 1993 *Rev. Mod. Phys.* **65** 1281
[11] Becklehimer J and Pandey R B 1992 *Physica* A **187** 71
[12] Cornette V, Ramirez-Pastor A J and Nieto F 2003 *Physica* A **327** 71
[13] Cornette V, Ramirez-Pastor A J and Nieto F 2003 *Eur. Phys. J.* B **36** 391
[14] Leroyer Y and Pommiers E 1994 *Phys. Rev.* B **50** 2795
[15] Bonnier B, Hontebeyrie M, Leroyer Y, Meyers C and Pommiers E 1994 *Phys. Rev.* E **49** 305
[16] Vandewalle N, Galam S and Kramer M 2000 *Eur. Phys. J.* B **14** 407
[17] Kondrat G and Pekalski A 2001 *Phys. Rev.* E **63** 051108
[18] Lebovka N I, Karmazina N N, Tarasevich Y Y and Laptev V V 2011 *Phys. Rev.* E **84** 061603
[19] Tarasevich Y Y, Lebovka N I and Laptev V V 2012 *Phys. Rev.* E **86** 061116
[20] Kondrat G 2005 *J. Chem. Phys.* **122** 184718
[21] Kondrat G 2006 *J. Chem. Phys.* **124** 054713
[22] Cornette V, Ramirez-Pastor A J and Nieto F 2006 *Phys. Lett.* A **353** 452
[23] Cornette V, Ramirez-Pastor A J and Nieto F 2006 *J. Chem. Phys.* **125** 204702
[24] Tarasevich Y Y, Laptev V V, Vygornitskii N V and Lebovka N I 2015 *Phys. Rev.* E **91** 012109
[25] Krapivsky P L, Redner S and Ben-Naim E 2010 *A Kinetic View of Statistical Physics* (New York: Cambridge University Press)
[26] García G D, Sanchez-Varretti F O, Centres P M and Ramirez-Pastor A J 2015 *Physica* A **436** 558
[27] Binder K 1997 *Rep. Prog. Phys.* **60** 488
[28] Yonezawa F, Sakamoto S and Hori M 1989 *Phys. Rev.* B **40** 636
[29] Hoshen J and Kopelman R 1976 *Phys. Rev.* B **14** 3428
[30] Biswas S, Kundu A and Chandra A K 2011 *Phys. Rev.* E **83** 021109
[31] Chandra A K 2012 *Phys. Rev.* E **85** 021149

J. Stat. Mech. (2015) P10011